International Journal of Nanomedicine

Dovepress
open access to scientific and medical research

Open Access Full Text Article

ORIGINAL RESEARCH

TET1-Lipid Nanoparticle Encapsulating Morphine for Specific Targeting of Peripheral Nerve for Pain Alleviation

Hongmei Yang[1,*], Zhongqi Liu[1,*], Fan Liu[1,2,*], Haixuan Wu[1], Xiaoyan Huang[1], Rong Huang[1], Phei Er Saw[3,4], Minghui Cao[1,2]

[1]Department of Anesthesiology, Sun Yat-Sen Memorial Hospital, Sun Yat-Sen University, Guangzhou, 510120, People's Republic of China; [2]Department of Anesthesiology, Shenshan Medical Center, Sun Yat-Sen Memorial Hospital, Sun Yat-sen University, Shanwei, 516600, People's Republic of China; [3]Medical Research Center, Sun Yat-Sen Memorial Hospital, Sun Yat-Sen University, Guangzhou, 510120, People's Republic of China; [4]Guangdong Provincial Key Laboratory of Malignant Tumor Epigenetics and Gene Regulation, Sun Yat-Sen Memorial Hospital, Sun Yat-Sen University, Guangzhou, 510120, People's Republic of China

*These authors contributed equally to this work

Correspondence: Phei Er Saw; Minghui Cao, Email caipeie@mail.sysu.edu.cn; caomh@mail.sysu.edu.cn

Background: Opioids are irreplaceable analgesics owing to the lack of alternative analgesics that offer opioid-like pain relief. However, opioids have many undesirable central side effects. Restricting opioids to peripheral opioid receptors could reduce those effects while maintaining analgesia.

Methods: To achieve this goal, we developed Tet1-LNP (morphine), a neural-targeting lipid nanoparticle encapsulating morphine that could specifically activate the peripheral opioid receptor in the dorsal root ganglion (DRG) and significantly reduce the side effects caused by the activation of opioid receptors in the brain. Tet1-LNP (morphine) were successfully prepared using the thin-film hydration method. In vitro, Tet1-LNP (morphine) uptake was assessed in differentiated neuron-like PC-12 cells and dorsal root ganglion (DRG) primary cells. The uptake of Tet1-LNP (morphine) in the DRGs and the brain was assessed in vivo. Von Frey filament and Hargreaves tests were used to assess the antinociception of Tet1-LNP (morphine) in the chronic constriction injury (CCI) neuropathic pain model. Morphine concentration in blood and brain were evaluated using ELISA.

Results: Tet1-LNP (morphine) had an average size of 131 nm. Tet1-LNP (morphine) showed high cellular uptake and targeted DRG in vitro. CCI mice treated with Tet1-LNP (morphine) experienced prolonged analgesia for nearly 32 h compared with 3 h with free morphine ($p < 0.0001$). Notably, the brain morphine concentration in the Tet1-LNP (morphine) group was eight-fold lower than that in the morphine group ($p < 0.0001$).

Conclusion: Our study presents a targeted lipid nanoparticle system for peripheral neural delivery of morphine. We anticipate Tet1-LNP (morphine) will offer a safe formulation for chronic neuropathic pain treatment, and promise further development for clinical applications.

Keywords: lipid nanoparticle, Tet1, peripheral nerve-targeted, pain management, chronic neuropathic pain

Introduction

Opioids remain the mainstay of analgesic treatment for perioperative, severe, acute, and chronic pain. However, opioid clinical effectiveness is restricted due to adverse side effects that are mainly caused by activating the μ-opioid receptors in the central nervous system (CNS),[1] including sedation, apnea, tolerance, and addiction which lead to an epidemic of overdoses, death, and abuse.[2] Therefore, there is an urgent need to develop novel therapeutic strategies for the management of pain. Currently, various approaches are being explored, including focusing on μ-opioid receptor (MOR) splice variants, generating biased agonists, or targeting other receptors such as heteromers with MOR.[3] Despite significant advances, clinical translation of these strategies remains challenging. Researchers have reduced opioid side effects by

Received: 23 January 2024
Accepted: 7 May 2024
Published: 27 May 2024

regulating transient receptor potential vanilloid 1 (TRPV1) receptors.[4] However, TRPV1 antagonists may increase the thermal pain threshold in humans, potentially increasing the risk of burn injury.[5]

As central effects account for the majority of opioid-related adverse effects, the use of opioid receptors only in peripheral sensory neurons is a promising therapeutic strategy to limit central adverse effects while maintaining analgesic effects.[3] There is growing evidence that peripheral sensory neurons mediate antinociceptive effects.[6,7] Primary sensory neurons, with cell bodies within dorsal root ganglia (DRGs), project fibers to the peripheral terminals of sensory neurons[8] and opioid receptors exist in DRG neurons of different diameters and prototypical sensory neuropeptides.[9] When there is a pain signal, opioid receptors are upregulated and transported through the axons of dorsal root ganglion (DRG) neurons to the peripheral terminals of sensory neurons.[10] Therefore, selective administration of opioids to peripheral sensory neurons and peripheral opioid receptor activation can result in analgesic effects. It has been reported that analgesia can be reduced through local administration of opioids, as demonstrated by intra-articular morphine.[11,12]

Although pharmacological, genetic, animal, and clinical studies have demonstrated that peripheral opioid receptors can mediate a significant portion of the analgesic effects produced by systemically administered opioids,[10,13–15] systemic delivery of morphine to peripheral neurons remains a challenge. Delivery methods based on nanotechnology appear promising. One of the most effective nanosystems with a wide range of clinical uses are liposomes and lipid-based nanovesicles.[16] By encapsulating opioids in nanoparticles, their molecular size can be significantly increased, while the passive diffusion of free drugs into the brain is decreased.

Unlike most of the neural targeting ligands discovered in current studies, which aimed to cross the blood-brain barrier (BBB)[17] and enter into the brain parenchyma[18] for brain disease treatment. Tet1 is a 12-amino acid peptide that has the binding characteristics of tetanus toxin targeting the trisialoganglioside (GT1b) receptor in neuronal cells and a strong affinity for differentiated PC-12 cells, primary motor neurons, and dorsal root ganglion cells.[19] Many researchers have studied and established the effectiveness of the neuronal targeting of Tet1.[19–24]

Herein, we developed a peripheral neural-targeting lipid nanoparticle (LNP) for activating opioid receptors in peripheral sensory neurons to limit central adverse effects while maintaining opioid analgesic effects. As shown in Figure 1, the nanoplatform is composed of a typical LNP structure, which involves a phospholipid bilayer surrounding an aqueous core, hydrophilic polyethylene glycol (PEG) chains on the outer shell, and Tet1 peptide to specifically target the peripheral nerve. The resulting nano platform displays the following unique functions after loading morphine and systemic administration: (i) large molecular size of encapsulated morphine is hardly to go through the blood-brain barrier (BBB); (ii) surface-modified peptide to specifically target the peripheral nerve, DRG, thus blocking ascending pathways transmission of the pain. With the release of the loaded drug, peripheral opioid receptors are activated and exhibit a strong and lasting analgesic effect.

Materials and Method

Materials

Lecithin and Coumarin-6 were acquired from Sigma–Aldrich. 1,2-Distearoyl-sn-glycero-3-phosphoethanolamine-N-(polyethylene glycol)-2000 (ammonium salt) (PEG_{2000}-DSPE), Scramble-PEG_{2000}-DSPE and Tet1-PEG_{2000}-DSPE were purchased from Tanshtech. Tet1 with the sequence HLNILSTLWKYRC, a scrambled peptide as a control with the sequence KRWYTNILHSLL, and Cy5.5-Tet1 were obtained from Tanshtech. Organic solvents (DMSO, DMF, and 75% ethanol) were purchased from Sigma-Aldrich and were used directly. Water was prepared using a Milli-Q system (Millipore®, Bedford, MA, USA). All other chemicals were of analytical grade and used without further purification.

Synthesis and Characterization of LNPs

Scramble-LNP (morphine) and Tet1-LNP (morphine), collectively denoted as LNPs (morphine), were prepared using a combination of the thin-film hydration method. Briefly, to synthesis of Scramble-LNP (morphine) or Tet1-LNP (morphine), lecithin was dissolved in chloroform and Scramble-PEG_{2000}-DSPE or Tet1-PEG_{2000}-DSPE (10wt% of the total lipid) was added. Chloroform was removed by rotary evaporation. Millipore grade water containing morphine was then added, and the resulting mixture (2 mg/mL) was briefly sonicated to accelerate the formation of morphine-loaded

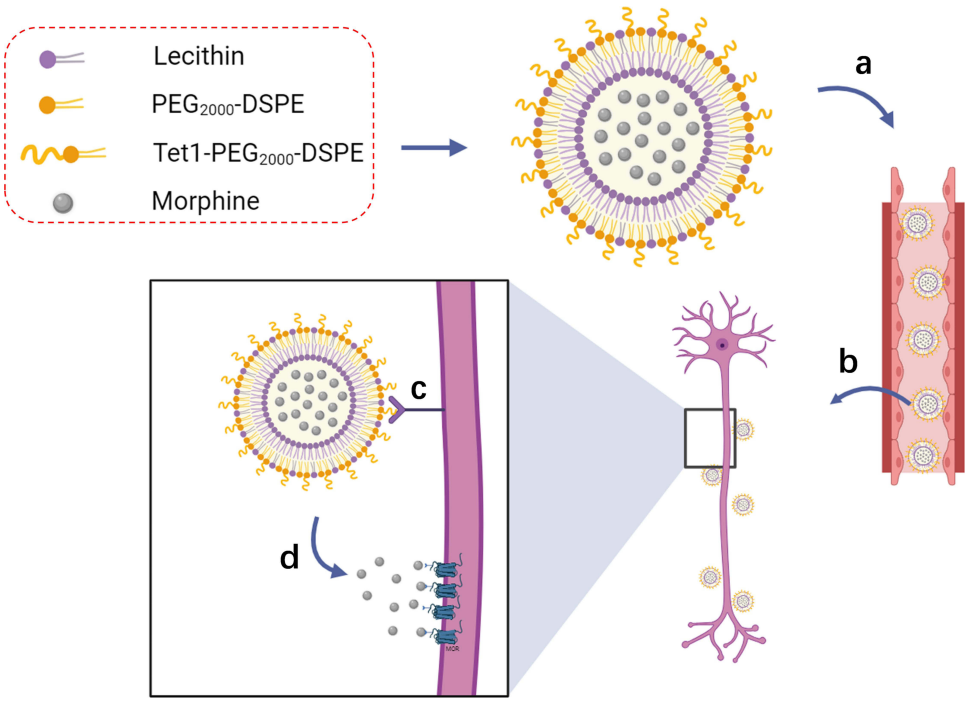

Figure 1 Formulation of the peptide-decorated lipid nanoparticle Tet1-LNP(morphine) and schematic illustration of the Tet1-LNP(morphine) for systemic morphine delivery and targeted pain treatment. After intravenous injection (**a**), the long-circulating Tet1-LNP (morphine) will not pass the BBB but target the neural cells via the specific recognition between peptide Tet1 and GT1b and accumulate in the peripheral nerve, DRG (**b**). After targeted cellular uptake (**c**), the Tet1-LNP (morphine) will release the morphine (**d**), leading to effective analgesia and limiting the side effects in the brain.

LNPs. The formed LNPs were transferred to an ultrafiltration device (EMD Millipore, MWCO 100K), centrifuged to remove free compounds, and dispersed in 1 mL of Phosphate buffer saline (PBS) solution.

Characterization of LNPs

The size and zeta potential of Scramble-LNP (morphine) and Tet1-LNP (morphine) were determined using Zetasizer nano ZS90 (Malvern Instruments, UK).[25] LNPs morphology were visualized using transmission electron microscopy (TEM; FEI Tecnai G2 12, Eindhoven, Netherlands).

Encapsulation Efficiency

The free morphine concentration was calculated based on its relative absorption value at 280 nm using a spectrophotometer (EVOLUTION201, Thermo Scientific, USA) equipped with matching quartz cells at a resolution of 1 nm from 260 nm to 350 nm. The concentration of morphine in the LNP sample was calculated using the non-encapsulated morphine in the ultrafiltration device. The encapsulation efficiency (EE) of morphine was calculated using the following equation.

EE% (morphine) = (M1 − M2) / M1 × 100%, where M1 and M2 are the masses of the initially added morphine and non-encapsulated morphine, respectively.

The structure of morphine prevents its coupling with fluorochromes. Hence, we substituted Coumarin-6 (C6), a fluorescent molecule with molecular weight similar to that of morphine. We calculated the EE of C6 in the Tet1-LNP (C6) or Scramble-LNP (C6) using the following formula:

$$\mathrm{EE\%\ (C6)} = (\mathrm{Amount\ of\ C6\ in\ LNPs\ (C6)} \,/\, \mathrm{initial\ amount\ of\ C6}\,) \times 100\%$$

Stability of LNPs

To determine the stability of the LNPs, we synthesized Tet1-LNP and Scramble-LNP, as mentioned above. The Tet1-LNP and Scramble-LNP were dissolved in PBS with 10% FBS to mimic physiological conditions. The vials were then kept in a 37°C chamber. At the indicated time points (1, 2, 4, 8, 18, and 24 h), the size of Tet1-LNP and Scramble LNP were assessed by DLS and recorded.

In vitro Release LNPs

Free C6, Scramble-LNP(C6), or Tet1-LNP (C6) (n = 3) was dispersed in 1 mL of PBS (pH 7.4), respectively and then transferred to a Spectra-Por® Float-A-Lyzer® G2 dialysis device (1mL, MWCO 100kDa, USA) that was immersed in PBS (pH 7.4) at 37°C. At the indicated time points (0, 0.25, 0.5, 1, 2, 3, 4, 6, 8, 10, 12, 24 h), 5 μL of the LNPs solution was collected from the inside of the dialysis device and added to 95 μL DMSO. After thorough mixing, the fluorescence intensity of C6 was determined using a multimode microplate reader (BioTek Synergy H1, Winooski, VT, USA).

Cell Culture

PC-12 and NIH-3T3 cells were purchased from Procell Life Science & Technology Co. Ltd. (CL-0481, CL-0171). The medium was changed every two days, and 10% Fetal Bovine serum (Gibco) and 1% penicillin and streptomycin (Gibco) were added. The Cells were maintained at 37 °C in a humidified cell culture chamber with 5% CO_2.

Primary DRG Isolation and Culture

C57BL/6J mice aged 3–4 weeks were sacrificed and sterilized by steeping in a 75% ethanol solution. After scissoring of the dorsal skin, the spine was completely removed and washed with PBS. Then, in a Petri dish containing cold 1 x HBSS, 1% penicillin, streptomycin, and 1% glucose, the spine was divided into two halves in midsagittal view. The DRGs were placed in cold 1× DMEM. The epineurium of the DRGs was carefully stripped using microsurgical forceps in cryic-DMEM, supplemented with 1% penicillin and streptomycin. The digested tissues were separated by trituration and placed on poly d-lysine-coated (Sigma, P7280) plates. The plating medium consisted of high-glucose Dulbecco's Modified Eagle's medium (DMEM, GIBCO) supplemented with 10% Fetal Bovine serum (FSP500, ExCell Biology) and 1% penicillin and streptomycin (Hyclone). After 24 h, the medium was replaced with Neurobasal medium (Invitrogen, 21,103,049) supplemented with B27 (Invitrogen, 17,504,044) and glutamine (Invitrogen, 25,030,081). Cultures were maintained at 37 °C in a humidified 5% CO_2 atmosphere. The medium was changed every two days.

In vitro Cellular Uptake of Tet1 Peptide and LNPs

PC-12 and NIH-3T3 cells were seeded at a density of 1×10^5 cells/well in 24-well plates. To label the cell membrane, the cells with wheat germ agglutinin (WGA) coupled to the Alexa Fluor™ 488 fluorochrome (Molecular Probes, Inc.) for 10 min at 37°C (5 μg/mL) and washed with 1×PBS three times to remove all the unbound WGA. Cy5.5-Tet1 was added to the culture medium and incubated for 15 min, 30 min, 1 h, 2 h. After incubation at 4 °C for indicated times, the samples were washed three times with PBS and fixed with 4% (w/v) paraformaldehyde (PFA). The nuclei were counterstained with 1 μg/mL DAPI (Sigma, D9542) for 15 min in the dark.

PC-12 and DRG cells were seeded at a density of 1×10^5 cells/well in a 24-well plate. To label the cell membrane, incubating cells with wheat germ agglutinin (WGA) coupled to the Texas Red™-X fluorochrome (Molecular Probes, Inc.) for 10 min at 37 °C (5 μg/mL) and washed with 1 × PBS three times to remove all the unbound WGA. Scramble-LNPs (C6) or Tet1-LNP (C6) were added to the culture medium and incubated for 15 min, 30 min, 1 h, 2 h. After incubation at 4 °C for indicated times, the samples were washed three times with PBS and fixed with 4% (w/v) paraformaldehyde (PFA). The nuclei were counterstained with 1 μg/mL DAPI (Sigma, D9542) for 15 min in the dark.

Flow Cytometry

PC-12 cells were seeded at a density of 1×10^5 cells/well in 24-well plates. Scramble-LNPs (C6) or Tet1-LNP (C6) were added to the culture medium. After 15 min, 30 min, 1 h, or 2 h incubation at 4 °C, the samples were washed with PBS

three times and fixed with 4% (w/v) paraformaldehyde (PFA). C6 intensity was quantified using a CytoFLEX flow cytometer (Beckman Coulter).

In vitro Cytotoxicity

PC-12 cells were seeded in 96-well plates at a density of 5000 cells per well. After incubation in 100 μL of culture medium for 24 h, a fixed amount of Scramble-LNP (morphine) or Tet1-LNP (morphine) was added to 100 mL of fresh medium and the cells were incubated for another 48 h. After replacing the medium with 100 μL of fresh culture medium, CCK-8 reagent was added to each well following the manufacturer's protocol. After incubation for 1 h at 450 nm, the absorbance was measured immediately, and cell viability was calculated.

Animals

Healthy male C57BL/6J normal mice (4–5 weeks old) were purchased from Zhuhai Bes Test Bio-Tech Co., Ltd. (Zhuhai, China). All in vivo studies were performed in accordance with a protocol approved by the Institutional Animal Care and Use Committee of the Sun Yat-sen Memorial Hospital Laboratory Animal Research Platform of Sun Yat-sen University in accordance with the principles outlined in the National Institutes of Health Guide for the Care and Use of Laboratory Animals. All mice were bred in the animal facility of the Laboratory Animal Research Platform of Sun Yat-sen Memorial Hospital, Sun Yat-sen University, and received free access to water and a routine mouse diet under a standard 12:12-h light-dark cycle in a room maintained at approximately 22 °C. The animal protocol was approved by Sun Yat-sen Memorial Hospital, Sun Yat-sen University Laboratory Animal Research Platform (AP20230082).

Pharmacokinetics

Healthy male C57BL/6J mice (6–8 weeks) were randomly divided into three groups (n = 3) and intravenously injected with free C6, Scramble-LNP (C6) or Tet1-LNP (C6). At specified time points, 20 μL of blood was collected and mixed with 80 μL of water. The fluorescence intensity of C6 in blood was determined using a multimode microplate reader (BioTek Synergy H1, USA).

Biodistribution

Free C6, Scramble-LNP (C6), or Tet1-LNP (C6) was intravenously (i.v.) injected into CCI C57BL/6J mice (n = 3 in each group) on day 7 after CCI surgery. The injection dosage was determined based on the dosage of C6 as 1 nmol). After 24 h, the mice were sacrificed, and the main organs, brain, and DRGs were obtained and observed using an IVIS® imaging system (Perkin Elmer, UK). The ImageJ software was used to quantify the fluorescence intensity of each tissue to measure accumulation in the brain, DRGs, and organs.

Immunofluorescence Staining

Experimental mice were anesthetized and cardiac perfusion was performed with 0.9% saline, followed by fixation with 4% paraformaldehyde (PFA). The Brains were quickly isolated and post-fixed in 4% PFA at 4 °C. After dehydration with 15% and 30% sucrose solutions, the brains were embedded in optimal cutting temperature medium (OCT; Sakura) and sectioned at a thickness of 25 μm. The brain slices were blocked and permeabilized in blocking buffer (1 × PBS containing 10% donkey serum and 0.3% Triton X-100) for 1 h. The following primary antibody and staining were used: mouse anti-NeuN (Millipore, MAB377, 1:200) overnight at 4 °C. The brain tissues were then incubated with Alexa Fluor 647-conjugated secondary antibodies (A11126, Invitrogen, 1:200) for 2 h at room temperature in the dark. The nuclei were counterstained with 1 μg/mL DAPI (Sigma, D9542) for 15 min in the dark. Images were obtained using a fluorescence microscope (IX73; Olympus).

DRGs were isolated and post-fixed in 4% PFA after perfusion. Then, 15% and 30% sucrose before inclusion with optimum cutting temperature reagent (OCT, Sakura) and 10 μm sections were cut in a cryostat and processed for immunofluorescence. After that, DRG slides were incubated with blocking buffer (PBS, 0.3% Triton) containing 3% bovine serum albumin (BSA) for 1 h and incubated with mouse anti-NeuN (Millipore, MAB377, 1:200) overnight (4 °C). The following day, the slides were washed and incubated with Alexa Fluor 647-conjugated secondary antibody (A11126,

Invitrogen, 1:200) for 2 h at room temperature in the dark. The nuclei were counterstained with 1 μg/mL DAPI (Sigma, D9542) for 15 min in the dark. Images were obtained using a fluorescence microscope (IX73; Olympus).

Chronic Constrictive Injury Pain Model

A chronic constrictive injury (CCI)-induced chronic neuropathic pain model was used, as previously described.[26] Briefly, under anesthesia, a 2-cm long blunt dissection is performed on the skin overlying the area between the gluteus and biceps femoris muscles, and expose the common sciatic nerve at the mid-thigh level, proximal to the trifurcation of the nerve. Approximately 7 mm of the common sciatic nerve was exposed at the mid-thigh level, and three loose ligatures (approximately 0.5 mm spacing) of 4–0 chromic guts around the sciatic nerve, until they elicited a brief twitch in the respective hind limbs. Therefore, it is important to avoid interrupting the epineural flow. Subcutaneous tissue and skin were sutured sequentially. The operation lasted for approximately 30 min. After recovery from anesthesia, the animals were returned to their cages and raised separately. In sham-operated animals, no ligatures were tied, which meant that sham animals, as controls, were only exposed to the sciatic nerve.

Behavioral Tests

All tests were performed during the light cycle between 8:00 a.m. and 8:00 P.M. Before testing each animal, the apparatus was thoroughly cleaned with 10% ethanol to reduce olfactory signals. To avoid the stress that comes with the new environment and adapt to the animals, starting 5 days before the test, the animals were placed in the test facility for 1 h per day to acclimate. Prior to the behavioral study, the mice were placed in their home cages in the room used for the experiment for 1 h on the day of testing.

Thermal Allodynia

Thermal hyperalgesia was tested according to the Hargreaves procedure,[27] slightly modified by us for the mouse. Briefly, mice were habituated to smaller clear plexiglass cubicles placed on an elevated glass platform, which was heated to 32°C (Plantar Test Analgesia Meter 390G, IITC Life Science). A constant intensity radiant heat source (beam diameter 0.5 cm and intensity, 25 I.R.) was used at the mid-plantar area of the hind paw. The paw withdrawal latency (PWLs) was recorded in seconds (s) as the interval between initial heat source activation and paw withdrawal from the target position. Each animal was tested six times per session, with at least 10 minutes of rest on the platform between measurements.

Mechanical Allodynia

Mechanical hyperalgesia was tested according to Zhang, Chi et al.[28] Briefly, mice were allowed to acclimate for 1 h. Two von Frey monofilaments (low-force, 0.07 g; high-force, 0.4 g) were used in the Paw withdrawal frequency (PWF) method to assess hypersensitivity to punctuate mechanical stimuli. Each von Frey filament was applied perpendicularly to the mid-plantar region of each hind paw for 1–2 s. The stimulation was repeated 10 times with at least a 5 min interval. The PWF was calculated as (number of paw withdrawals/10 trials) ×100%.

ELISA Assay for Morphine Concentration

To directly examine the concentration of morphine released from LNPs compared to that of free morphine, we collected blood and brain samples of CCI mice at the indicated time points (1, 3, 5, 8, 24, and 48 h) after the injection of free morphine, Scramble-LNP (morphine), and Tet1-LNP (morphine). Free morphine, Scramble-LNP (morphine), and Tet1-LNP (morphine) had the same absolute quantities as morphine (3 mg/kg).

Under deep isoflurane anesthesia, blood samples were obtained by the intracardiac puncture, transferred to ice, and spun down at 4 °C and 3000 rpm for 15 min. The supernatant (plasma) was collected and stored at 80 °C immediately after centrifugation. After blood collection, cardiac perfusion was performed using 0.9% saline solution.

To collect brain samples, the mice were perfused with saline under deep isoflurane anesthesia. The brains were removed and stored at −80°C. After thawing, approximately 250 mg of the brain into a 1.5 mL centrifuge tube, and added 750 μL RIPA Buffer containing protease inhibitors was added. The tissue was then homogenized and sonicated on ice. Centrifuge The tube at 1600 x g for 10 min at 4°C.

All plasma and brain samples from mice were purified and processed according to the manufacturer's instructions (Cayman NO.501940). To maintain the range of the standard curve, some samples (thawed blood plasma) were diluted 1:1000 with Immunoassay Buffer C from the ELISA kit. The absorbance measurements were immediately read at a wavelength of 450 nm, and morphine concentration was calculated accordingly.

Histology

At the end of the evaluation period, the mice in each group were sacrificed after the treatment, and the brain, DRGs, and main organs (heart, liver, spleen, lungs, and kidneys) were collected. After fixation with 4% paraformaldehyde and embedding in paraffin, the tissue was sectioned, stained with hematoxylin and eosin (H&E), and viewed using an optical microscope.

Statistical Analysis

Statistical analysis was performed using Prism 9.5 software (GraphPad Software, United States). The differences between two groups were analyzed using 2-tailed, unpaired Student's *t*-test, unpaired *t*-test with Welch's correction, or the Mann–Whitney test. Parametric data were analyzed using 2-tailed, unpaired Student's *t*-test, or a 1-way or 2-way ANOVA followed by the post hoc Tukey's test for multiple comparisons, and nonparametric data were analyzed using the Scheirer-Ray-Hare test. Statistical significance was set at $p < 0.05$.

Results

Preparation and Characterizations of LNPs

To examine the effect of the Tet1 peptide on the cellular and DRG uptake of LNPs in vitro and in vivo, we prepared Tet1 peptide-modified LNP and Scramble peptide-modified LNP as control. These two LNPs were prepared using a combination of the thin-film hydration method and were used for morphine delivery, denoted as Tet1-LNP (morphine) and Scramble-LNP (morphine). The surface of the lecithin bilayer can form hydrogen bonds or electrostatic interactions with the morphine aqueous solution, thereby encapsulating the drug in the hydrophilic core of the LNP. Hydrophilic polyethylene glycol (PEG) chains and Tet1 peptide were on the outer shell of LNP. Figure 1 shows a schematic representation of Tet1-LNP (morphine). The Tet1-LNP (morphine) showed spherical morphology with an average size of ~ 131 nm, as determined by DLS (Figure 2A). Compared with the empty Tet1-LNP (~110 nm, Figure 2B), there was an increase of approximately 20 nm after morphine was loaded. mV, both indicated negative charge, Tet1-LNP (blank) as −27.4 mV ± 1.84 mV and Tet1-LNP (morphine) as −25.75 mV ± 1.76 mV (Figure 2C and D).

Scramble-LNP (morphine) and Tet1-LNP (morphine) showed similar encapsulation efficacy to morphine, while Tet1-LNP (morphine) exhibited a higher encapsulation ability of morphine (Tet1-LNP: 38%; Scramble-LNP: 35%). According to the TEM results, Scramble-LNPs (morphine) and Tet1-LNP (morphine) were spherical in shape and had an average size of approximately 120 nm (Figure 2E and F). To check whether the LNPs were stable, their sizes were measured using DLS. The results are shown in Figure 2G, where the diameter of the LNPs was stable at approximately 120 nm when incubated in 10% FBS-containing phosphate buffer solution (PBS) solution for 24 h.

The release profile of LNPs were determined by encapsulation of Coumarin-6 (C6). Results showed that Tet1-LNP (C6) and Scramble-LNP (C6) released only approximately 10%, whereas free C6 released approximately 40% within the first four hours. During the subsequent 20 h, free C6 slowly released 95% of the C6. At the same time, the C6 release profile indicated that Tet1-LNP (C6) and Scramble-LNP (C6) released only approximately 25% (Figure 2H).

In vitro Neural Targeting of Peptide Tet1

The in vitro neural targeting ability of Tet1 was first evaluated by examining the uptake of Cy5.5-Tet1 by PC-12 cells, which have been widely used as a neuronal line study model,[29] and NIH-3T3 cells, which is the embryonic mouse fibroblast cell line.[30] The representative fluorescent images were shown in Figure 3A and B. Compared to NIH-3T3 cells, the cellular uptake of Cy5.5-Tet1 in PC-12 cells is much higher in different incubation times (Figure 3C), proving the neural targeting ability of the Tet1 peptide.

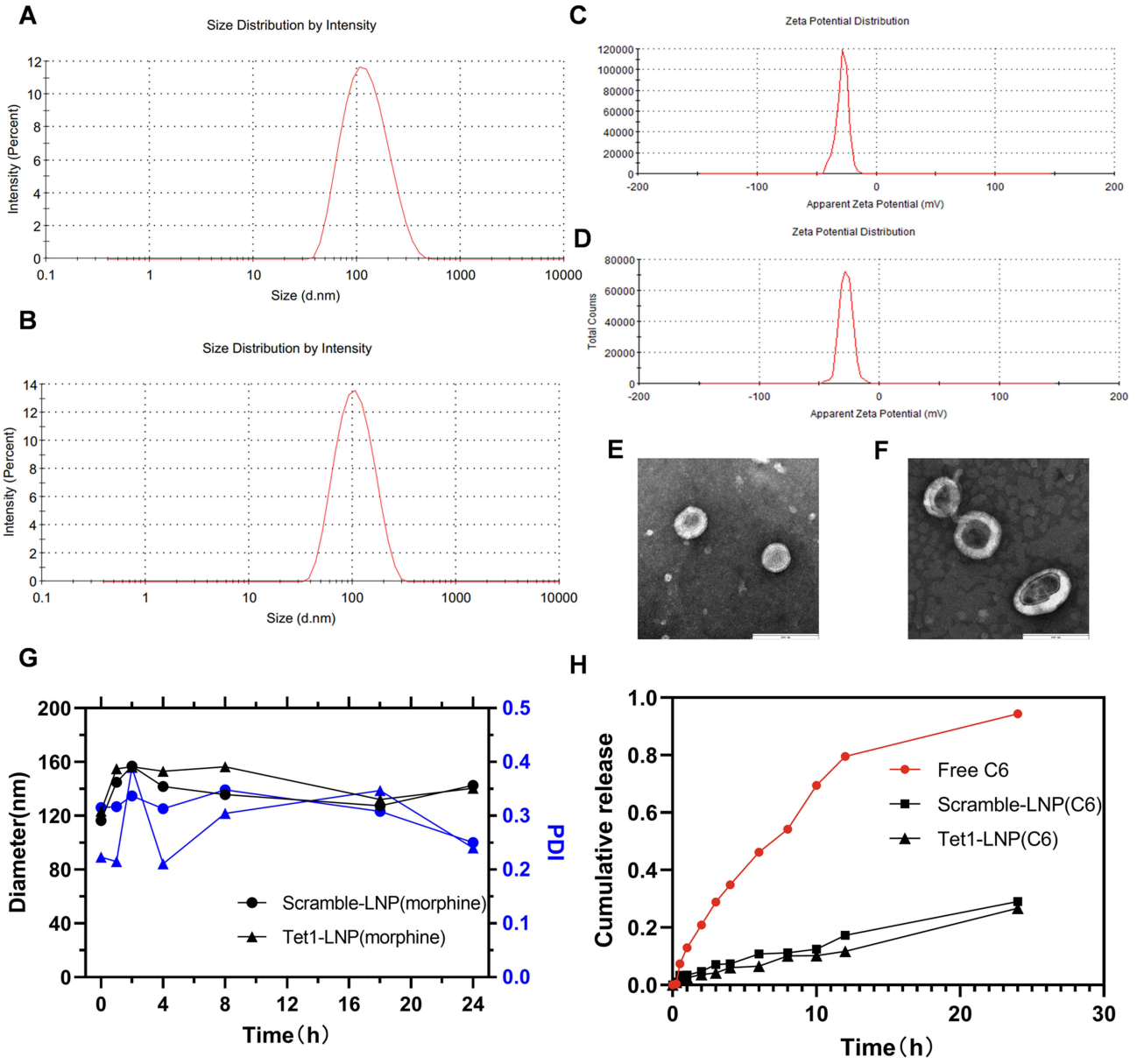

Figure 2 Characterization of LNPs. (**A**) Size distribution of Tet1-LNP(morphine). (**B**) Size distribution of Tet1-LNP(blank). (**C**) Zeta potential of Tet1-LNP(blank). (**D**) Zeta potential of Tet1-LNP (morphine). TEM image of (**E**) Scramble-LNPs (morphine) and (**F**) Tet1-LNP(morphine). (**G**) Size and polydispersity (PDI) of the Tet1-LNP(morphine) or Scramble-LNP(morphine) incubated in PBS buffer containing 10% FBS for different times. (**H**) In vitro release profile of free Coumarin-6 (C6), Scramble-LNP (C6), and Tet1-LNP (C6) incubated in PBS buffer at 37 °C.

In vitro Neural Targeting of Tet1-LNP

The in vitro neural targeting ability of Tet1-LNP was evaluated by examining the uptake of Tet1-LNP (C6) by PC-12 cells (Figure 4A) and the primary DRG (Figure 4B). Due to the presence of specific recognition between Tet1 and neural cells, the cellular uptake of Tet1-LNP (C6) is much higher than Scramble-LNP (C6), both in PC-12 cells ($p < 0.05$) and DRGs ($p < 0.0001$) (Figure 4C and D). Quantitative analysis using flow cytometry further supported the neural-targeting ability of Tet1-LNP. As shown in Figure 5A and B, Tet1 decoration resulted in a 2-fold increase in cellular uptake ($p < 0.001$). These results suggested that Tet1-LNP exhibited good neural-targeting ability in vitro.

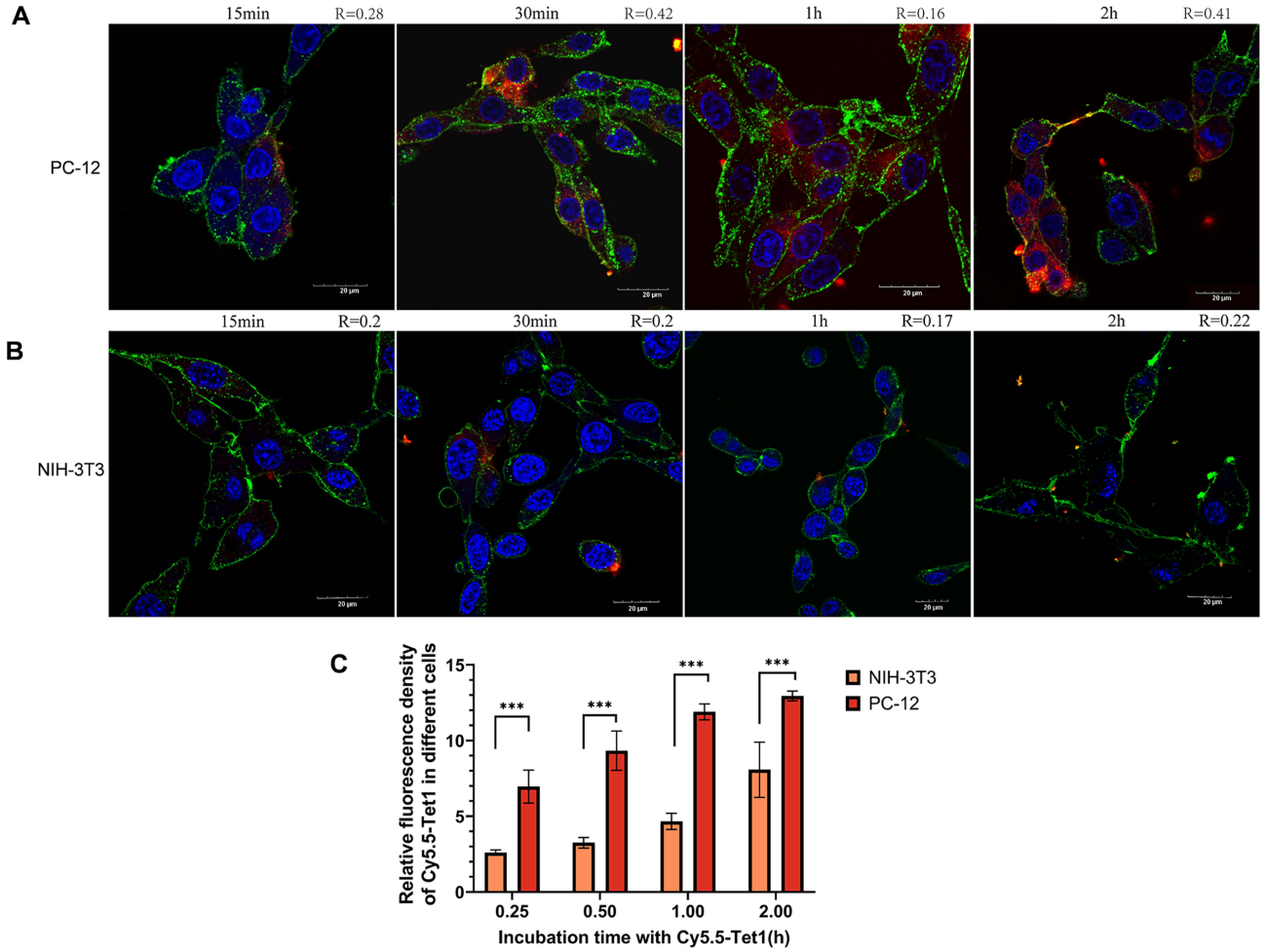

Figure 3 FV3000 confocal laser scanning microscope image of the PC-12 cells(**A**) and NIH-3T3 cells (**B**) incubated with Cy5.5-Tet1 peptide for 15 min, 30 min, 1 h and 2 h. The nuclei, cell membrane, and Cy5.5-Tet1 were stained by blue, green, and red fluorescence, respectively. (Scale bar = 20 μm) (**C**) Quantification of the data shown in (**A**) and (**B**). n = 3 per group. ***$p < 0.001$ by one-way analysis of variance (ANOVA).

In vitro and in vivo Toxicity of Tet1-LNP

To investigate the in vitro neural cell growth inhibition ability of LNPs, PC-12 cells were treated with different concentrations of free morphine, blank LNPs, and morphine-loaded LNPs for 24h before cell viability was measured. As shown in Figure 5C, free morphine, blank LNPs, and morphine-loaded LNPs did not significantly inhibit the growth of PC-12 cells at concentrations ranging from 0.005 μM to 1 μM.

To further evaluate in vivo safety, the LNPs were injected intravenously at a dose of 3 mg/kg per mouse into C57 mice. After 24 h, the major organs were taken for H&E staining to investigate the tissue damage. Compared with the control group, H&E staining showed no noticeable histological changes in the tissues, including the heart, liver, spleen, lung, or kidney of LNP-treated mice (Figure 6), revealing that Tet1-LNP is safe in vivo. In addition, our immunofluorescence staining results showed that LNPs were not toxic to neurons, as the staining distribution of NeuN, which labels neurons, did not change in C57 mice treated with LNPs (Figure 8A and B).

Pharmacokinetics and in vivo Targeting Efficacy of Tet1-LNP

To evaluate the circulation stability of LNPs, we investigated their pharmacokinetics. As shown in Figure 7A, after intravenous injection, the Scramble-LNP (C6) and Tet1-LNP (C6) groups both showed long blood circulation times with a half-life (t1/2) of ~7 h, which was far longer than that of the free C6 group (t1/2 ~30 min).

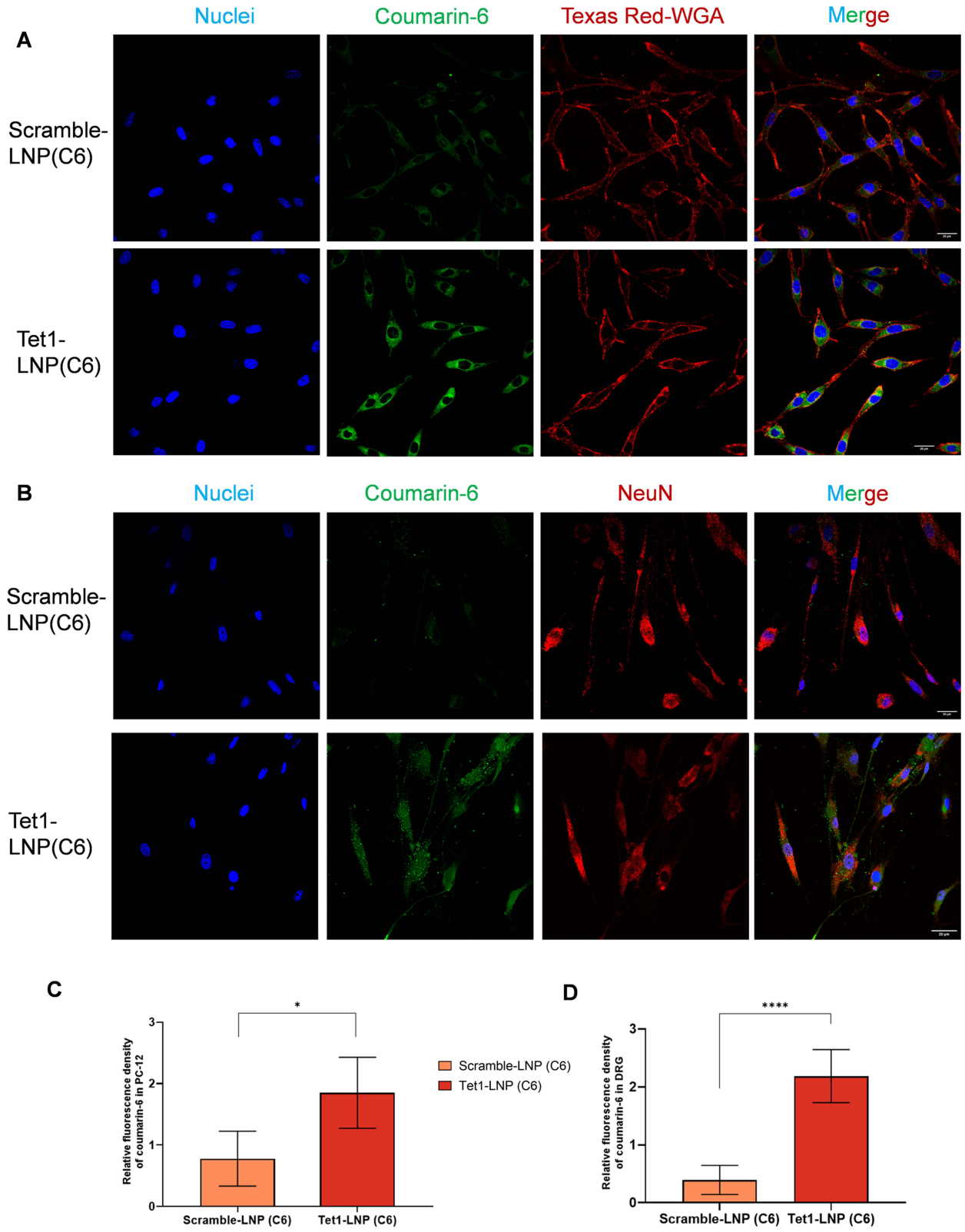

Figure 4 FV3000 confocal laser scanning microscope image of the PC-12 cells (**A**) and DRG cells (**B**) incubated with the Scramble-LNP (C6) or the Tet1-LNP (C6) on ice for 1 h. The nuclei, coumarin-6 were respectively stained by blue and green. (Scale bar =20 μm) (**A**) PC-12 cell membrane was stained by red fluorescence. (**B**) NeuN was stained by red fluorescence in DRG. Quantification of the relative fluorescence density of Coumarin-6 in PC-12 cells (**C**) and DRG (**D**). (n = 3, *$p < 0.05$, ****$p < 0.0001$).

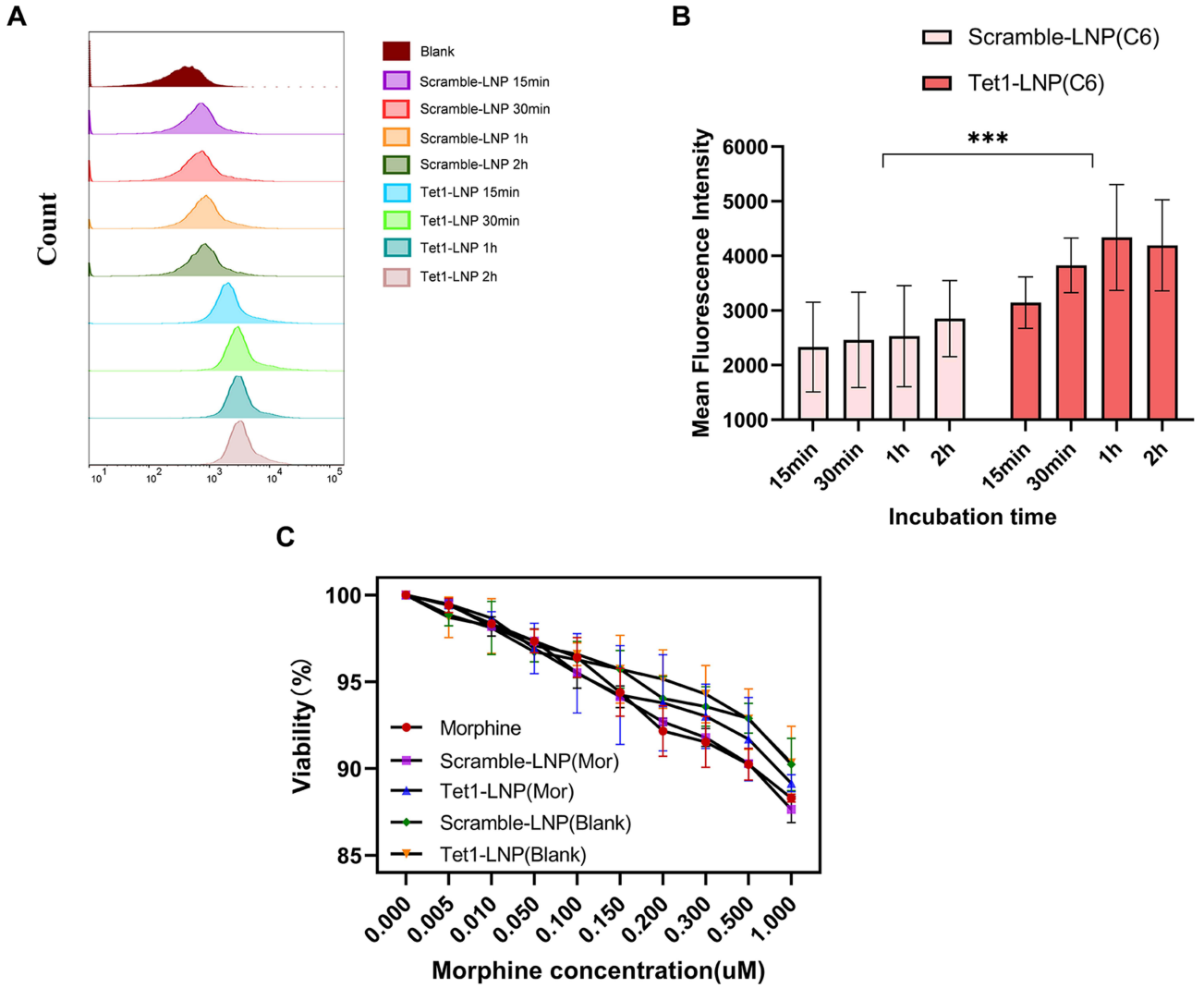

Figure 5 Cellular uptake and cytotoxicity of LNPs. (**A**) Flow cytometry analysis of PC-12 cells incubated with the Scarmble-LNP (C6) or the Tet1-LNP (C6) on ice for 15 min, 30 min, 1 h, 2 h. (**B**) Mean fluorescence intensity (MFI). (n = 3, ***$p < 0.001$) (**C**) In vitro cytotoxicity assay to observe the PC-12 cells killing ability of Morphine, Scramble-LNP, Tet1-LNP, Scramble-LNP (Morphine) and Tet1-LNP (Morphine), respectively.

After validating the in vitro neural-targeting ability of Tet1-LNP, we evaluated the in vivo peripheral neural-targeting ability of this nanoplatform. To further investigate the biodistribution of LNPs and the in vivo neural targeting ability, C6 was loaded into Scramble-LNP and Tet1-LNP, and intravenously injected into C57 mice on day 7 after chronic constrictive injury (CCI) surgery. The brains, DRGs, and main organs were harvested at 24 h post-injection. As shown in Figure 7B, the Tet1-mediated neural targeting, Tet1-LNP (C6) group showed a much higher accumulation of DRGs than the free C6 group ($p < 0.001$, n = 3) or Scramble-LNP (C6) group ($p < 0.001$, n = 3), whereas the Tet1-LNP (C6) group accumulated less C6 in the brain than the free C6 group ($p < 0.01$, n = 3). Compared to the free C6 group, the Scramble-LNP (C6) group also accumulated less C6 in the brain ($p < 0.05$, n = 3). The fluorescent image of the main organs of the mice was showed in Figures 7C.

Immunofluorescence staining analysis of the brains (Figure 8A) and DRGs (Figure 8B) also supported the peripheral neuron-targeting ability of Tet1-LNP, and the fluorescence of the Tet1-LNP (C6) group accumulated more in DRGs than in the free C6 group ($p < 0.001$, n = 3) and Scramble-LNP (C6) group ($p < 0.0001$, n = 3) (Figure 8C), but less in the brain than that of the free C6 group ($p < 0.01$, n = 3) (Figure 8D). The Scramble-LNP (C6) group also accumulated less fluorescence in the brain than did the free C6 group ($p < 0.05$, n = 3) (Figure 8D).

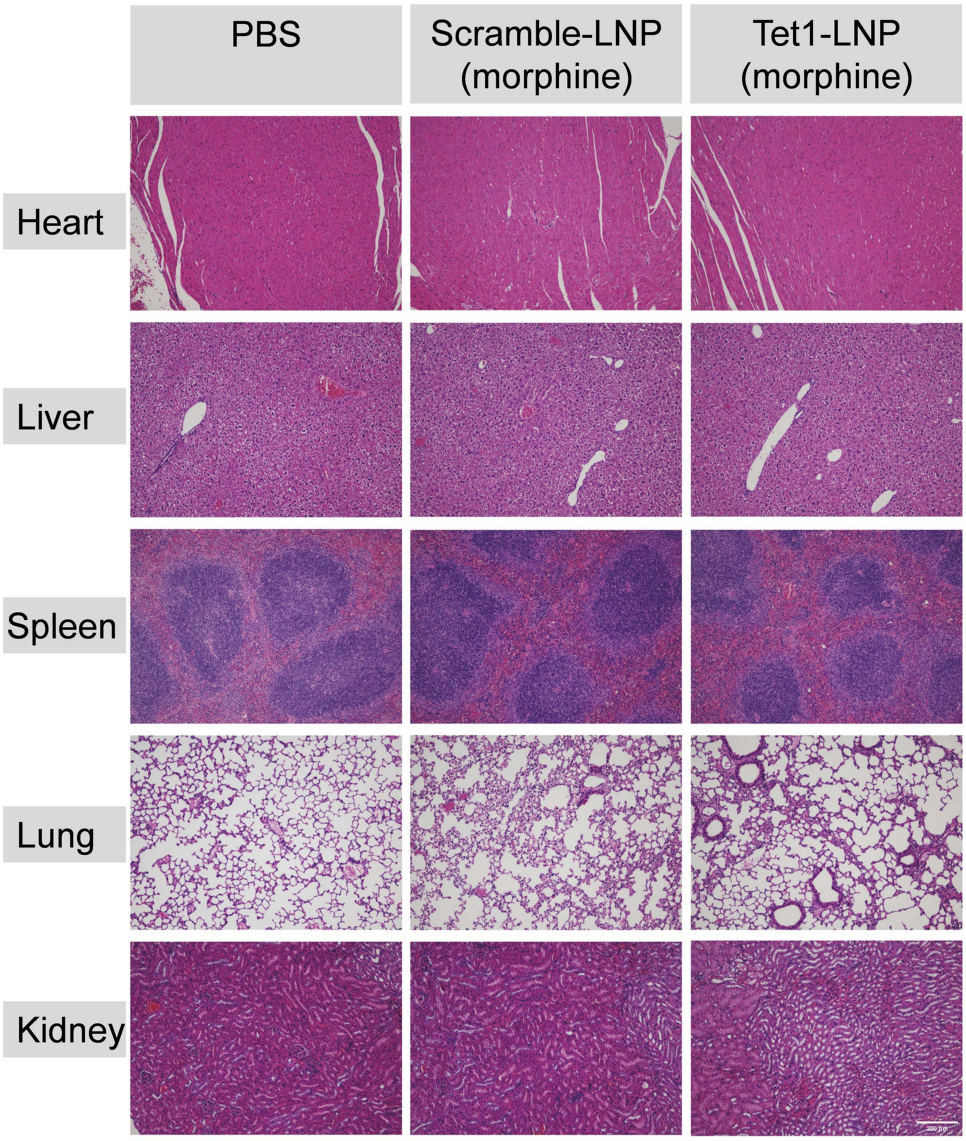

Figure 6 Histological analysis of tissue sections of main organs. Histological sections of the major organs, including heart, liver, spleen, lung and kidney of the mice after systemic treatment of the PBS, Scramble-LNP (morphine), and Tet1-LNP (morphine). Hematoxylin-eosin. (scale bar = 200 μm).

Analgesic Effect Assessment

As shown in Figure 9A, the mice were taken 1-hour adaption to the test environment for five days before CCI or sham surgery. CCI was induced by loose ligation of the sciatic nerve using three 4/0 chromic silk sutures. CCI mice exhibited a significant decrease in thermal paw withdrawal latencies (PWLs) in the affected hind paws; however, this decrease was absent in sham-surgery animals (Figure S1A in Supporting information). A significant increase in the mechanical paw withdrawal frequency (PWF) was observed in the affected hind paws, whereas this increase was absent in sham-treated animals (Figure S1B and S1C in Supporting information). To assess the analgesic effect, on day 7 after CCI surgery, after measuring the PWLs and PWF, free morphine, Scramble-LNP (morphine), and Tet1-LNP (morphine) were intravenously injected into mice that underwent CCI or sham surgery. The dosages were calculated to contain the same absolute quantity of morphine (3 mg/kg), and the amount of morphine in the LNPs(morphine) was quantified by spectrophotometry. Thermal hyperalgesia and mechanical hyperalgesia behavioral tests were taken 1 h, 3 h, 5 h, 8 h, 24 h, 32 h, 48 h after injection.

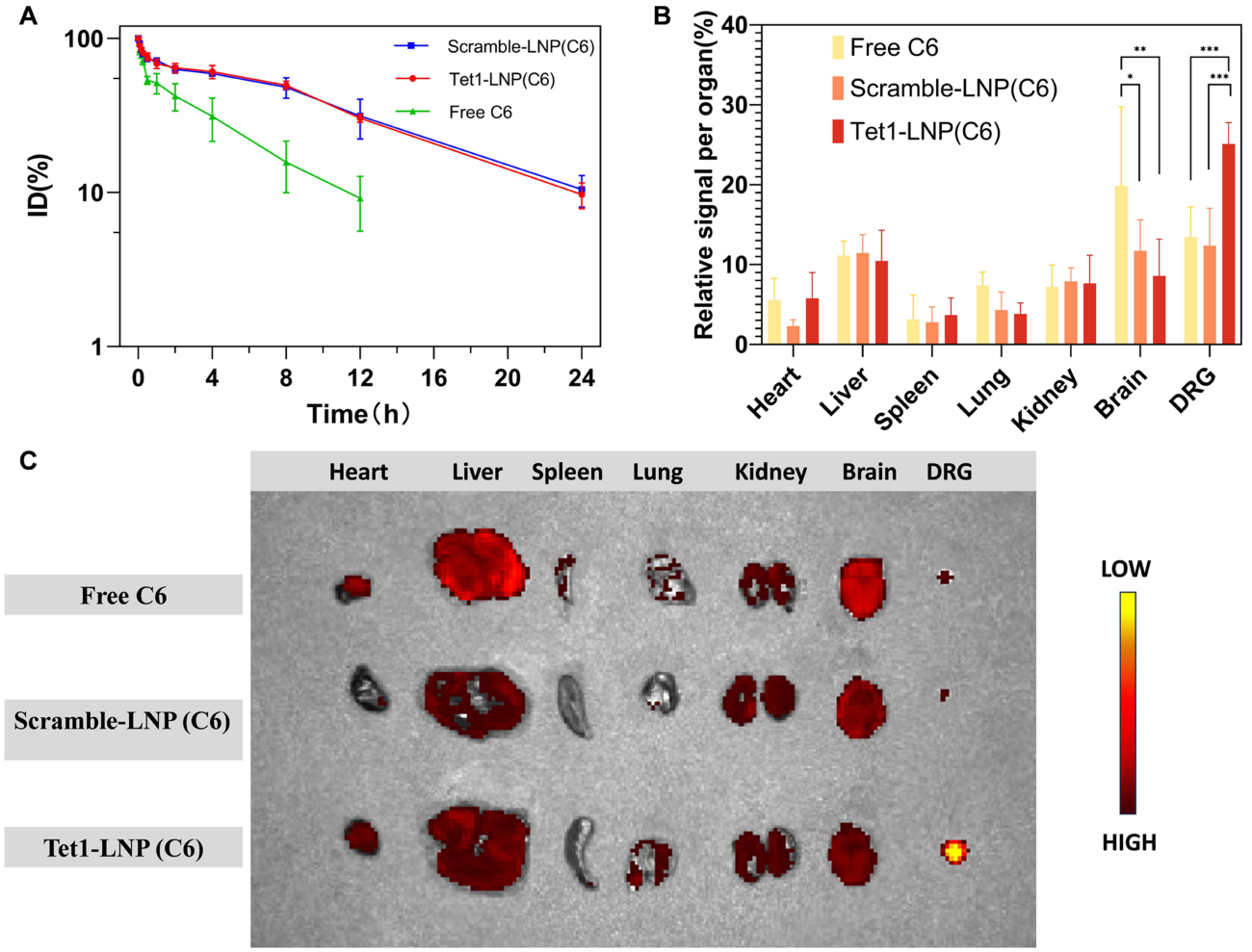

Figure 7 Pharmacokinetics of LNPs. The circulation time of Tet1-LNP(C6) and Scramble (C6) after i.v. injection to mice via the tail vein. (**A**) Blood circulation profile of C57 mice of the free Coumarin-6 group, the Scramble-LNP (C6) group, and the Tet1-LNP (C6) group. (**B**) Quantification of the data obtained from (**C**). (**C**) Overlaid fluorescent image of the main organs of the mice after respectively i.v. injection of free Coumarin-6, the Scramble-LNP (C6) or the Tet1-LNP (C6) 24 h. (n = 3, * $p < 0.05$, ** $p < 0.01$, *** $p < 0.001$).

As shown in Figure 9B, PWLs of the CCI group after thermal stimuli were significantly increased within 5 h after the injection of free morphine, scramble-LNP (morphine), and Tet1-LNP (morphine), whereas PWLs of sham-operated mice did not increase after injection. In the CCI mice group, the analgesia of the LNPs groups were significantly longer than that of the free morphine group. In particular, the PWLs of the Tet1-LNP (morphine) group were notably longer, for almost 32 h, while PWLs of the free morphine group turned out to be the same as before the injection after 5 h.

In sham operation group, 0.07 g PWF and 0.4 g PWF showed no obvious increase after the injection of free morphine and LNPs (morphine) (Figure 9C and D). As for mechanical hyperalgesia in the CCI group, the 0.07 g PWF of free morphine was significantly decreased within 5 h after the injection, whereas 0.07 g PWF of the Scramble-LNP (morphine) group decreased within 24 h, and that of the Tet1-LNP (morphine) group decreased for 32 h (Figure 9C). Furthermore, 0.4 g PWF of the free morphine group only decreased within 3 h after injection, when 0.4 g PWF of Scramble-LNP (morphine) group decreased for 24 h and the Tet1-LNP (morphine) group decreased for 32 h (Figure 9D). Moreover, 0.4 g PWF of the Tet1-LNP (morphine) group showed a noticeable decrease from 8 to 32 h after administration compared with that of the Scramble-LNP (morphine) group ($p < 0.05$; Figure 9D). These results suggest that Tet1-LNP (morphine) could induce better thermal and mechanical analgesia and last longer than free morphine and Scramble-LNP (morphine).

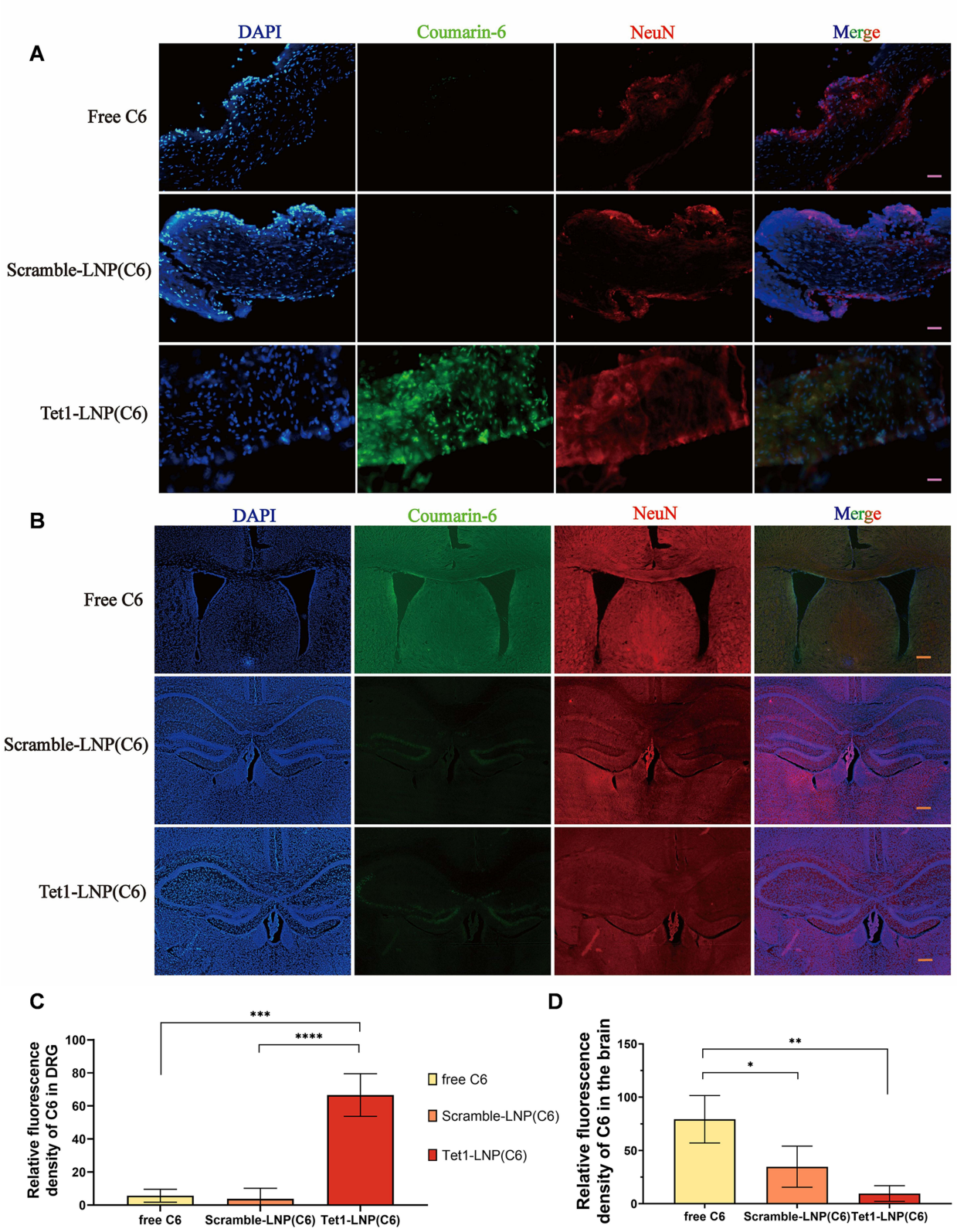

Figure 8 In vivo neural targeting ability of Tet1-LNP (C6) after intravenous injection to mice. (**A**) Fluorescent images of DRGs at 24 h post-injection of free Coumarin-6, the Scramble-LNP (C6) or the Tet1-LNP (C6). (purple scale bar = 50 μm). (**B**) Fluorescent images of brains at 24 h post-injection of free Coumarin-6, the Scramble-LNP (C6) or the Tet1-LNP (C6). (Orange scale bar = 100 μm). The nuclei, Coumarin-6, and neurons were stained by blue, green, and red fluorescence, respectively. The quantification of the relative fluorescence density of Coumarin-6 in DRGs (**C**) and brains (**D**). (n = 3, * $p < 0.05$, ** $p < 0.01$, *** $p < 0.001$, **** $p < 0.0001$).

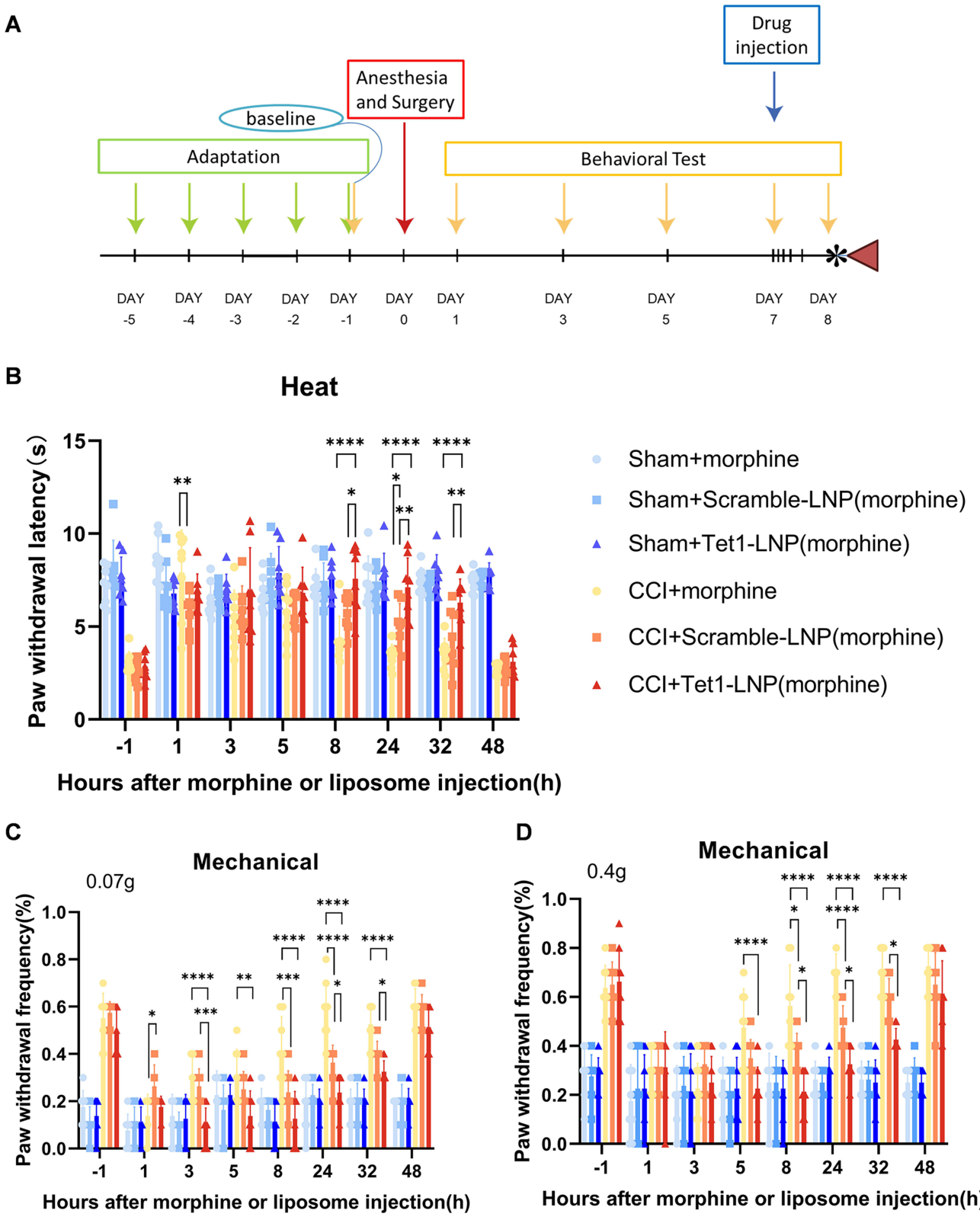

Figure 9 Effect of morphine and morphine LNPs in mice with or without CCI surgery. 7 days after CCI or sham operation, mice were tested for baseline (−1 h time point). Then, they received morphine, the Scramble-LNP (morphine), or the Tet1-LNP (morphine) injection, respectively. (3 mg/kg, i.v.) (**A**) Schematic illustration and timeline for the behavioral test and treatment. Paw withdrawal latencies to heat (**B**), paw withdrawal frequencies to 0.07g Von Frey filaments (**C**), and paw withdrawal frequencies to 0.4 g Von Frey filaments (**D**) were examined on 1, 3, 5, 8, 24, 32, and 48 hours after the injection. (n = 8 mice per group, * $p < 0.05$, ** $p < 0.01$, *** $p < 0.001$, **** $p < 0.0001$).

https://doi.org/10.2147/IJN.S453608 DovePress

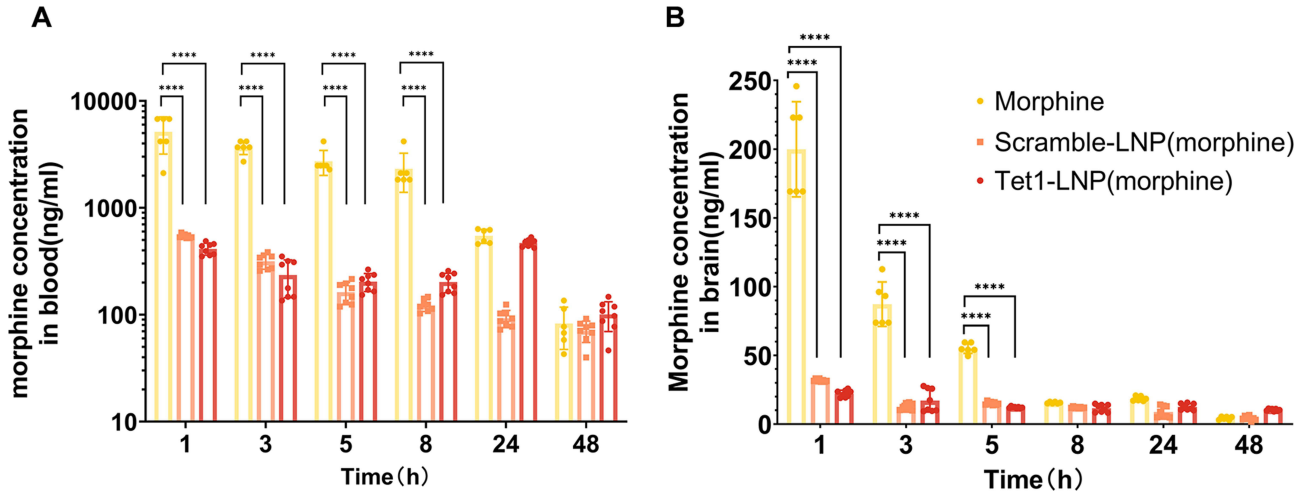

Figure 10 Concentrations of free morphine in blood (**A**) and brain (**B**). After i.v. injection of morphine (n = 6) or the Scramble-LNP (morphine) (n = 8) or Tet1-LNP (morphine), respectively. (equivalent to 3 mg/kg free morphine, **** $p < 0.0001$).

In vivo Concentrations of Free Morphine in Circulating Blood, and Brain

We obtained blood and brain samples from CCI mice at designated times to directly compare the amount of morphine released from LNPs to that of free morphine. Morphine concentrations were determined using an enzyme-linked immunosorbent assay (ELISA). All the samples were purified and processed according to the manufacturer's instructions. As shown in Figure 10A, the mean peak morphine concentration in blood for the free morphine group was 6780 ng/mL, 586 ng/mL for the Scramble-LNP (morphine) group, and 489 ng/mL for the Tet1-LNP (morphine) group. We then examined the mean peak morphine concentration in the brain. The mean peak concentrations of morphine are up to 246 ng/mL in morphine group, while 32 ng/mL for Scramble-LNP (morphine) group and 28 ng/mL Tet1-LNP (morphine) group (Figure 10B). The Tet1-LNP (morphine) group concentration of morphine in the brain is eightfold lower morphine concentration in that of the free morphine group. These results suggest that the Tet1-LNP (morphine) platform developed in this study can be used as a safe and efficient pain treatment method.

Discussion

Opioids are vital treatments for chronic pain owing to their powerful analgesic effects. However, the use of opioid drugs is restricted because of side effects, such as addiction, tolerance, and respiratory depression, which result from the activation of μ-opioid receptors (MORs) in particular brain regions.[31,32] As pain can be effectively inhibited by activating peripheral opioid receptors,[15,33] we synthesized LNPs to deliver morphine towards peripheral opioid receptors and avoid the side effects of opioid receptor activation in the brain.

LNPs are the most common carriers for drug delivery, allowing drugs to accumulate in target tissues, while minimizing systemic toxicity, and LNPs are unable to cross the BBB and enter the brain due to their large size (100 nm).[34,35] In our research, we successfully kept morphine outside of the brain as the size of the Tet1-LNP (morphine) was averaged out to 131 nm. By encapsulating inside the LNPs, morphine will not be non-specific uptake into the brain, reducing the passive diffusion of free morphine.[36] Our data showed that, after intravenous injection of Tet1-LNP (morphine), morphine barely crossed the brain (Figures 8B and 10B). At the same time, the size of Tet1-LNP (morphine) is above the kidney filtration threshold (approximately 10 nm) to reduce the obstacle of renal excretion,[37] and a diameter of less than 200 nm might reduce activation of the complement system and prolong circulation time.[38] Tet1-LNP (morphine) are ideal for stability, good loading capacity, and low BBB penetration.

In the peripheral nervous system, opioid receptor expression has been demonstrated in nerve terminals, peripheral axons, and nociceptive neurons in the dorsal root ganglia (DRG).[39] The presence of these receptors suggests the potential significance of the peripheral nervous system in analgesic effects. Recently, a novel 12-amino-acid peptide, Tet1, has been found capable of competing with tetanus toxin for trisialoganglioside (GT1b) receptor binding and has been

successfully used as a molecular conjugate to target neurons.[19,20] In this study, Tet1-mediated peripheral nerve targeting by nanoparticles was demonstrated in vitro (Figure 4B) and in vivo (Figures 7C and 8A), which is consistent with previous studies.[19,20] In contrast to previous studies that employed Tet1-modified nanoparticles to construct a targeted delivery system for CNS tissues,[40] this indicates that after modification by the Tet1 peptide, the Tet1-LNP (morphine) mainly targets towards peripheral nerves, rather than entering the brain. In addition, this system may be utilized in studies related to the peripheral mechanisms of neuropathic pain. In our study, Tet1-LNP (morphine) was harmless both in vitro and in vivo, which is in accordance with the fact that lipid nanoparticles have already established clinical safety for in vivo application.[41]

Our data showed that after intravenous injection, the Tet1-LNP (morphine) group showed good analgesia in CCI mice while maintaining a longer analgesic time than the free morphine group according to the behavioral test (Figure 9B–D). These results indicate that in the chronic neuropathic pain model, after intravenous injection of Tet1-LNP (morphine), morphine was slowly released into the targeted tissue, DRG, and accumulated, leading to a solid and prolonged analgesic effect. Our findings are consistent with previous studies demonstrating that tissue injury, such as inflammation or neuropathy, increases the analgesic efficacy of peripheral opioids.[42] The powerful analgesic effect may be due to the upregulation, accessibility, and increased functionality of peripheral opioid receptors, consistent with numerous experimental and clinical studies that have suggested that analgesic effects also arise from the activation of peripheral neuronal opioid receptors.[10,14,15,43–45] In addition, the Tet1-LNP (morphine) group exhibited lower peripheral blood and morphine concentrations in the brain (Figure 9B), which could not only reduce the central side effects of morphine but also avoid potential side effects acting on peripheral non-neural tissue opioid receptors. Furthermore, it is necessary to investigate the abuse potential of Tet1-LNP (morphine) in detail.

This study had certain limitations that may require further research. Firstly, although our experiments suggest that morphine in the Tet1-LNP (morphine) group spares across the brain, additional approaches, such as head-out plethysmography to noninvasively monitor lung function, are needed to further confirm that Tet1-LNP (morphine) can limit the side effects of opioid-induced respiratory depression. In addition, further research is required to determine how blocking peripheral receptors produces a stronger analgesic effect. The specific milieu of inflamed tissue has been reported to increase the efficacy of opioid agonists by enhancing G-protein coupling and increasing neuronal cyclic adenosine monophosphate (cAMP) levels.

In summary, we developed a morphine-loaded Tet1 peptide-modified lipid nanoparticle system. Our in vitro findings suggest that Tet1-LNP (morphine) exhibits long-lasting stability, high peripheral nerve targeting, and is harmless. In the CCI model, Tet1-LNP (morphine) had good analgesia, lasted for a long time, and hardly entered the brain, with minimal central side effects. Taken together, Tet1-LNP (morphine) could potentially be used as an alternative opioid analgesic and could be easily translated into clinical applications. In addition, this system may be utilized in studies related to the peripheral mechanisms of neuropathic pain.

Funding

This work was supported by the "Three million for Three Years" Project of the Academic Backbone of Shenshan Medical Center, Sun Yat-Sen Memorial Hospital (China) and the Natural Science Foundation of Guangdong Province, China (Grant No. 2022A1515010612). The authors thank the Yichang Humanwell Pharmaceutical Co. Ltd. for supporting this project.

Disclosure

The authors declare no conflicts of interest in this work.

References

1. Cohen SP, Vase L, Hooten WM. Chronic pain: an update on burden, best practices, and new advances. *Lancet*. 2021;397(10289):2082–2097. doi:10.1016/s0140-6736(21)00393-7
2. Benyamin R, Trescot AM, Datta S, et al. Opioid complications and side effects. *Pain Physician*. 2008;11(2 Suppl):S105–20.

3. Busserolles J, Lolignier S, Kerckhove N, Bertin C, Authier N, Eschalier A. Replacement of current opioid drugs focusing on MOR-related strategies. *Pharmacol Ther*. 2020;210:107519. doi:10.1016/j.pharmthera.2020.107519
4. Wang X, Bao C, Li Z, Yue L, Hu L. Side effects of opioids are ameliorated by regulating trpv1 receptors. *Int J Environ Res Public Health*. 2022;19 (4):2387.
5. Chung MK, Wang S. Cold suppresses agonist-induced activation of TRPV1. *Journal of Dental Research*. 2011;90(9):1098–1102. doi:10.1177/0022034511412074
6. Baron R, Hans G, Dickenson A. Peripheral input and its importance for central sensitization. *Ann Neurol*. 2013;74(5):630–636. doi:10.1002/ana.24017
7. Richards N, McMahon S. Targeting novel peripheral mediators for the treatment of chronic pain. *Br J Anaesth*. 2013;111(1):46–51. doi:10.1093/bja/aet216
8. Mélik Parsadaniantz S, Rivat C, Rostène W, Réaux-Le Goazigo A. Opioid and chemokine receptor crosstalk: a promising target for pain therapy? *Nat Rev Neurosci*. 2015;16(2):69–78. doi:10.1038/nrn3858
9. Busch-Dienstfertig M, Stein C. Opioid receptors and opioid peptide-producing leukocytes in inflammatory pain--basic and therapeutic aspects. *Brain Behav Immun*. 2010;24(5):683–694. doi:10.1016/j.bbi.2009.10.013
10. Stein C, Machelska H. Modulation of peripheral sensory neurons by the immune system: implications for pain therapy. *Pharmacol Rev*. 2011;63 (4):860–881. doi:10.1124/pr.110.003145
11. Zeng C, Gao S, Cheng L, et al. Single-dose intra-articular morphine after arthroscopic knee surgery: a meta-analysis of randomized placebo-controlled studies. *Arthroscopy*. 2013;29(8):1450–8.e2. doi:10.1016/j.arthro.2013.04.005
12. Stein C, Comisel K, Haimerl E, et al. Analgesic effect of intraarticular morphine after arthroscopic knee surgery. *New Engl J Med*. 1991;325 (16):1123–1126. doi:10.1056/nejm199110173251602
13. Labuz D, Mousa S, Schäfer M, Stein C, Machelska H. Relative contribution of peripheral versus central opioid receptors to antinociception. *Brain Res*. 2007;1160:30–38. doi:10.1016/j.brainres.2007.05.049
14. Gaveriaux-Ruff C, Nozaki C, Nadal X, et al. Genetic ablation of delta opioid receptors in nociceptive sensory neurons increases chronic pain and abolishes opioid analgesia. *Pain*. 2011;152(6):1238–1248. doi:10.1016/j.pain.2010.12.031
15. Jagla C, Martus P, Stein C. Peripheral opioid receptor blockade increases postoperative morphine demands--a randomized, double-blind, placebo-controlled trial. *Pain*. 2014;155(10):2056–2062. doi:10.1016/j.pain.2014.07.011
16. Sercombe L, Veerati T, Moheimani F, Wu SY, Sood AK, Hua S. Advances and challenges of liposome assisted drug delivery. *Front Pharmacol*. 2015;6:286. doi:10.3389/fphar.2015.00286
17. Liang M, Gao C, Wang Y, et al. Enhanced blood-brain barrier penetration and glioma therapy mediated by T7 peptide-modified low-density lipoprotein particles. *Drug Delivery*. 2018;25(1):1652–1663. doi:10.1080/10717544.2018.1494223
18. van Rooy I, Mastrobattista E, Storm G, Hennink W, Schiffelers R. Comparison of five different targeting ligands to enhance accumulation of liposomes into the brain. *J Control Release*. 2011;150(1):30–36. doi:10.1016/j.jconrel.2010.11.014
19. Park I, Lasiene J, Chou S, Horner P, Pun S. Neuron-specific delivery of nucleic acids mediated by Tet1-modified poly(ethylenimine). *J Genet Med*. 2007;9(8):691–702. doi:10.1002/jgm.1062
20. Liu J, Teng Q, Garrity-Moses M, et al. A novel peptide defined through phage display for therapeutic protein and vector neuronal targeting. *Neurobiol Dis*. 2005;19(3):407–418. doi:10.1016/j.nbd.2005.01.022
21. Zhang Y, Zhang W, Johnston AH, Newman TA, Pyykkö I, Zou J. Targeted delivery of Tet1 peptide functionalized polymersomes to the rat cochlear nerve. *Int j Nanomed*. 2012;7:1015–1022. doi:10.2147/IJN.S28185
22. Federici T, Liu J, Teng Q, Yang J, Boulis N. A means for targeting therapeutics to peripheral nervous system neurons with axonal damage. *Neurosurgery*. 2007;60(5):911–8; discussion−8. doi:10.1227/01.Neu.0000255444.44365.B9
23. Kwon E, Lasiene J, Jacobson B, Park I, Horner P, Pun S. Targeted nonviral delivery vehicles to neural progenitor cells in the mouse subventricular zone. *Biomaterials*. 2010;31(8):2417–2424. doi:10.1016/j.biomaterials.2009.11.086
24. Wang P, Zheng X, Guo Q, et al. Systemic delivery of BACE1 siRNA through neuron-targeted nanocomplexes for treatment of alzheimer's disease. *J Control Release*. 2018;279:220–233. doi:10.1016/j.jconrel.2018.04.034
25. Liang M, Guo M, Saw PE, Yao Y. Fully natural lecithin encapsulated nano-resveratrol for anti-cancer therapy. *Int j Nanomed*. 2022;17:2069–2078. doi:10.2147/ijn.S362418
26. Martucci C, Trovato A, Costa B, et al. The purinergic antagonist PPADS reduces pain related behaviours and interleukin-1 beta, interleukin-6, iNOS and nNOS overproduction in central and peripheral nervous system after peripheral neuropathy in mice. *Pain*. 2008;137(1):81–95. doi:10.1016/j.pain.2007.08.017
27. Hargreaves K, Dubner R, Brown F, Flores C, Joris J. A new and sensitive method for measuring thermal nociception in cutaneous hyperalgesia. *Pain*. 1988;32(1):77–88. doi:10.1016/0304-3959(88)90026-7
28. Zhang C, Hu MW, Wang XW, et al. scRNA-sequencing reveals subtype-specific transcriptomic perturbations in DRG neurons of Pirt(EGFPf) mice in neuropathic pain condition. *eLife*. 2022;11. doi:10.7554/eLife.76063
29. Oprea D, Sanz CG, Barsan MM, Enache TA. PC-12 cell line as a neuronal cell model for biosensing applications. *Biosensors*. 2022;12(7):500.
30. Rahimi AM, Cai M, Hoyer-Fender S. Heterogeneity of the NIH3T3 fibroblast cell line. *Cells*. 2022;11(17):2677.
31. Pattinson KT. Opioids and the control of respiration. *Br J Anaesth*. 2008;100(6):747–758. doi:10.1093/bja/aen094
32. Volkow ND, Morales M. The brain on drugs: from reward to addiction. *Cell*. 2015;162(4):712–725. doi:10.1016/j.cell.2015.07.046
33. Bagues A, Martín MI, Higuera-Matas A, Esteban-Hernández J, Ambrosio E, Sánchez-Robles EM. Mu-opioid receptors in ganglia, but not in muscle, mediate peripheral analgesia in rat muscle pain. *Anesthesia Analg*. 2018;126(4):1369–1376. doi:10.1213/ane.0000000000002717
34. Morse SV, Mishra A, Chan TG, TMdR R, Choi JJ. Liposome delivery to the brain with rapid short-pulses of focused ultrasound and microbubbles. *J Control Release*. 2022;341:605–615. doi:10.1016/j.jconrel.2021.12.005
35. Shishi H, Yanni F, Zicong T, et al. Optimization of ultra-small nanoparticles for enhanced drug delivery. *BIO Integration*. 2023;4(2):62–69. doi:10.15212/bioi-2022-0015
36. Groenendaal D, Freijer J, de Mik D, Bouw MR, Danhof M, de Lange EC. Population pharmacokinetic modelling of non-linear brain distribution of morphine: influence of active saturable influx and P-glycoprotein mediated efflux. *Br J Pharmacol*. 2007;151(5):701–712. doi:10.1038/sj.bjp.0707257

37. Peng C, Huang Y, Zheng J. Renal clearable nanocarriers: overcoming the physiological barriers for precise drug delivery and clearance. *J Control Release*. 2020;322:64–80. doi:10.1016/j.jconrel.2020.03.020
38. Faraji A, Wipf P. Nanoparticles in cellular drug delivery. *Bioorg Med Chem*. 2009;17(8):2950–2962. doi:10.1016/j.bmc.2009.02.043
39. Zhang X, Bao L, Li S. Opioid receptor trafficking and interaction in nociceptors. *Br J Pharmacol*. 2015;172(2):364–374. doi:10.1111/bph.12653
40. Mathew A, Fukuda T, Nagaoka Y, et al. Curcumin loaded-PLGA nanoparticles conjugated with Tet-1 peptide for potential use in Alzheimer's disease. *PLoS One*. 2012;7(3):e32616. doi:10.1371/journal.pone.0032616
41. Khare P, Edgecomb SX, Hamadani CM, Tanner EEL, Sm D. Lipid nanoparticle-mediated drug delivery to the brain. *Adv Drug Delivery Rev*. 2023;197:114861. doi:10.1016/j.addr.2023.114861
42. Stein C, Schäfer M, Machelska H. Attacking pain at its source: new perspectives on opioids. *Nature Med*. 2003;9(8):1003–1008. doi:10.1038/nm908
43. Spahn V, Del Vecchio G, Labuz D, et al. A nontoxic pain killer designed by modeling of pathological receptor conformations. *Science*. 2017;355(6328):966–969. doi:10.1126/science.aai8636
44. Stein C. Opioid Receptors. *Annu Rev Med*. 2016;67:433–451. doi:10.1146/annurev-med-062613-093100
45. Weibel R, Reiss D, Karchewski L, et al. Mu opioid receptors on primary afferent nav1.8 neurons contribute to opiate-induced analgesia: insight from conditional knockout mice. *PLoS One*. 2013;8(9):e74706. doi:10.1371/journal.pone.0074706